iScience, Volume *23*

Supplemental Information

PPARα Ligand-Binding Domain Structures with Endogenous Fatty Acids and Fibrates

Shotaro Kamata, Takuji Oyama, Kenta Saito, Akihiro Honda, Yume Yamamoto, Keisuke Suda, Ryo Ishikawa, Toshimasa Itoh, Yasuo Watanabe, Takahiro Shibata, Koji Uchida, Makoto Suematsu, and Isao Ishii

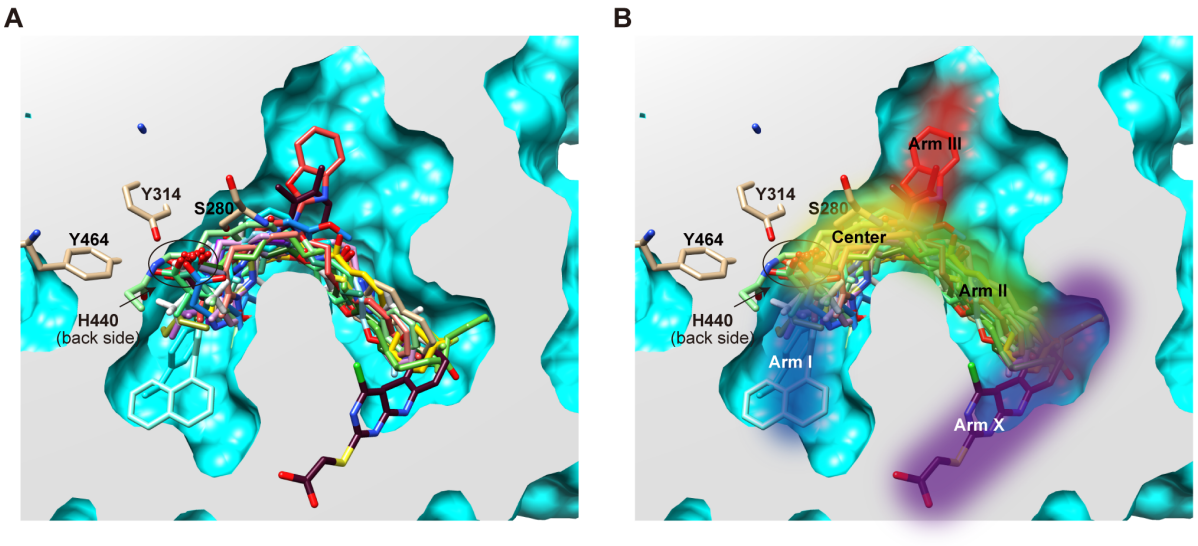

Figure S1. Twenty-one PPARα ligands located in PPARα-LBD, Related to Figures 1–4

(A) Twenty-one PPARα ligands, including 20 agonists and 1 antagonist, located in PPARα-LBD in the PDB registered crystal structures. (B) Five regions of PPARα-LBD (Arm I–III and X, and Center). A binding site for carboxylic residues common to PPARα ligands (*circled*) is surrounded by four amino acids (S280, Y314, H440, and Y464) and located between Arm I and Center regions. Pemafibrate is located deep in Arm III with its benzoxazole ring (*red*) (Kawasaki *et al.*, 2020), and one of the two Wy14643 molecules is found to be located in Arm X (Bernardes *et al.*, 2013). Only two ligands, 2-methyl-2-[4-(naphthalen-1-yl)phenoxy]propanoic acid and (2S,3S)-1-(4-methoxyphenyl)-3-(3-(2-(5-methyl-2-phenyloxazol-4-yl)ethoxy)benzyl)-4-oxoazetidine-2-carboxyl ic acid (65W and REW, respectively, in Table S1), are located in Arm I.

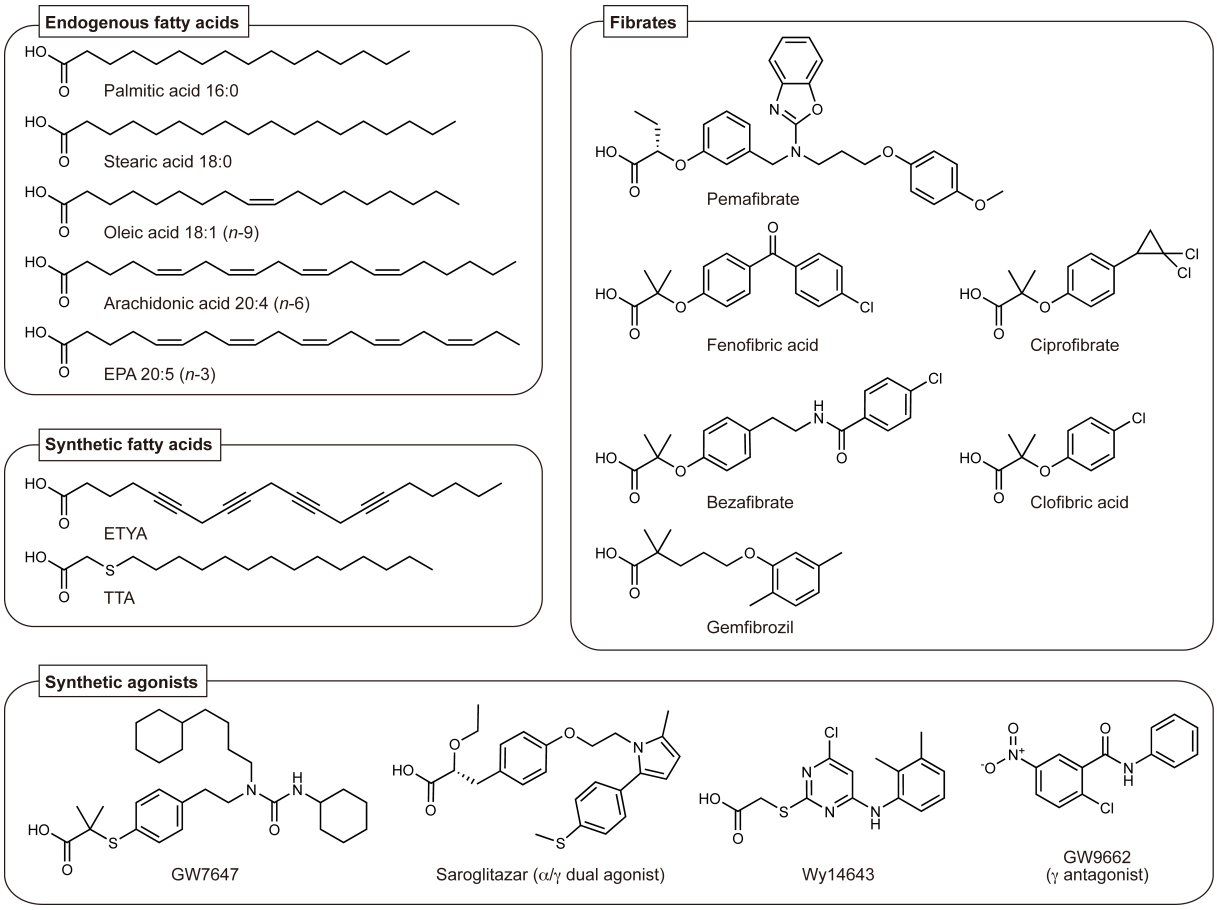

Figure S2. Chemical structures of 17 PPARα ligands analyzed in this study, Related to Figure 1
Five endogenous fatty acids, including EPA, two synthetic fatty acids (ETYA, 5,8,11,14-eicosatetraynoic acid [arachidonic acid mimetic]; TTA, tetradecylthioacetic acid, which is a PPAR pan agonist), six clinically approved fibrates, and four synthetic agonists, including saroglitazar, which is a PPARα/γ dual agonist, and GW9662, which is a PPARγ-selective antagonist.

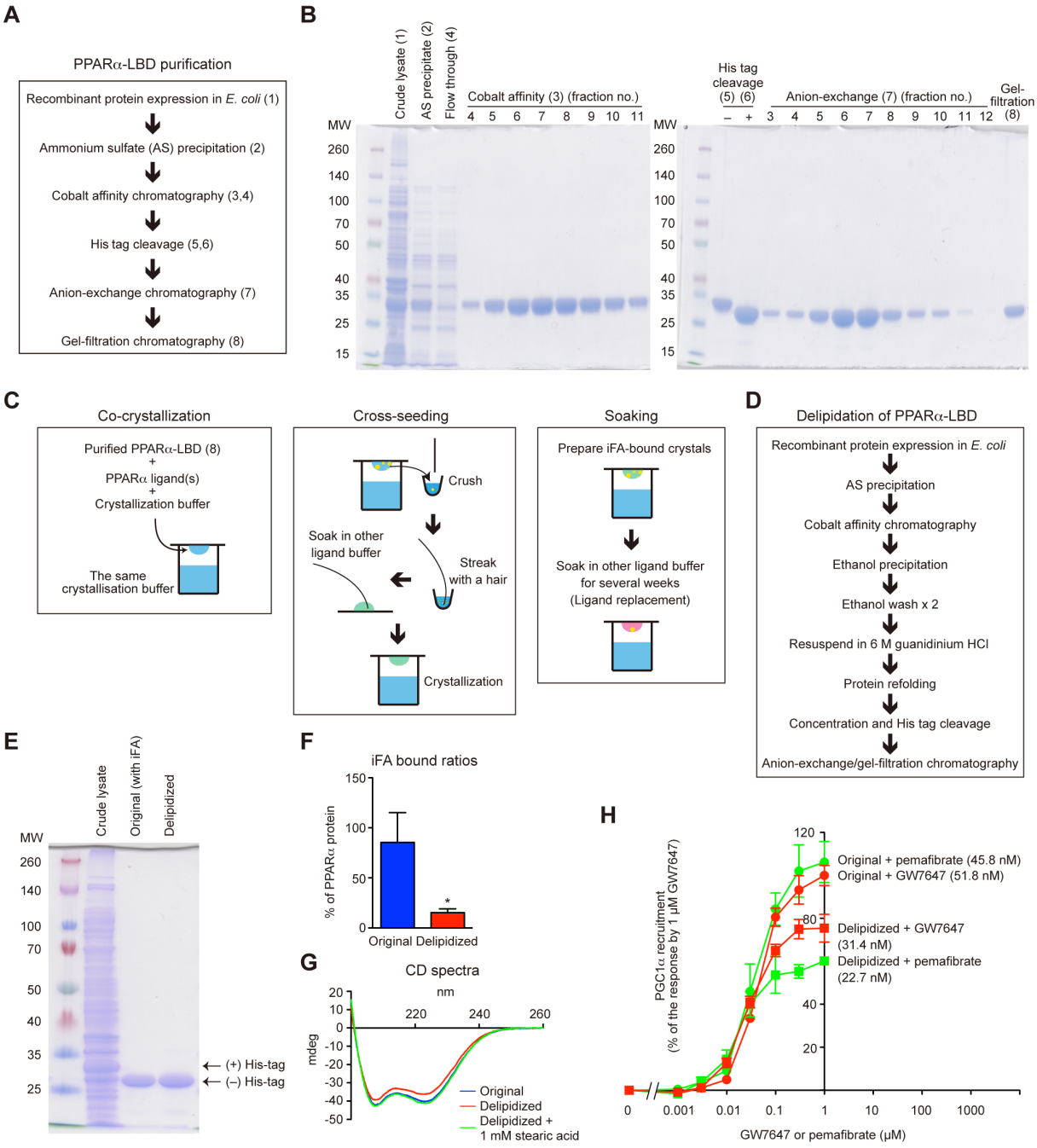

Figure S3. Methods for purification, delipidation, and crystallization of human PPARα-LBD proteins, and a functional assay of delipidized proteins, Related to Figure 1

(A, B) Methods (A) and SDS-PAGE gel check (B) of three-step chromatography for PPARα-LBD purification. (C) The different crystal preparation methods used in this study: co-crystallization, cross-seeding, and soaking. (D) Delipidation procedures to remove intrinsic fatty acid (iFA). (E) SDS-PAGE gel check of delipidized PPARα-LBD. (F–H) Comparative analyses of original and delipidized PPARα-LBD using iFA-bound ratios (F), circular dichroism (CD) spectra (G), PPARα activation (PGC1α recruitment) by agonists (H). The difference is significant ($^{*}P<0.05$) in (F). Stearic acid supplementation (1 mM) restored the CD spectrum shift by delipidation in (G). Similar EC_{50} values (in parentheses) were obtained from pemafibrate/GW7647 concentration-dependent activation of original (iFA-bound) and delipidized PPARα-LBD proteins.

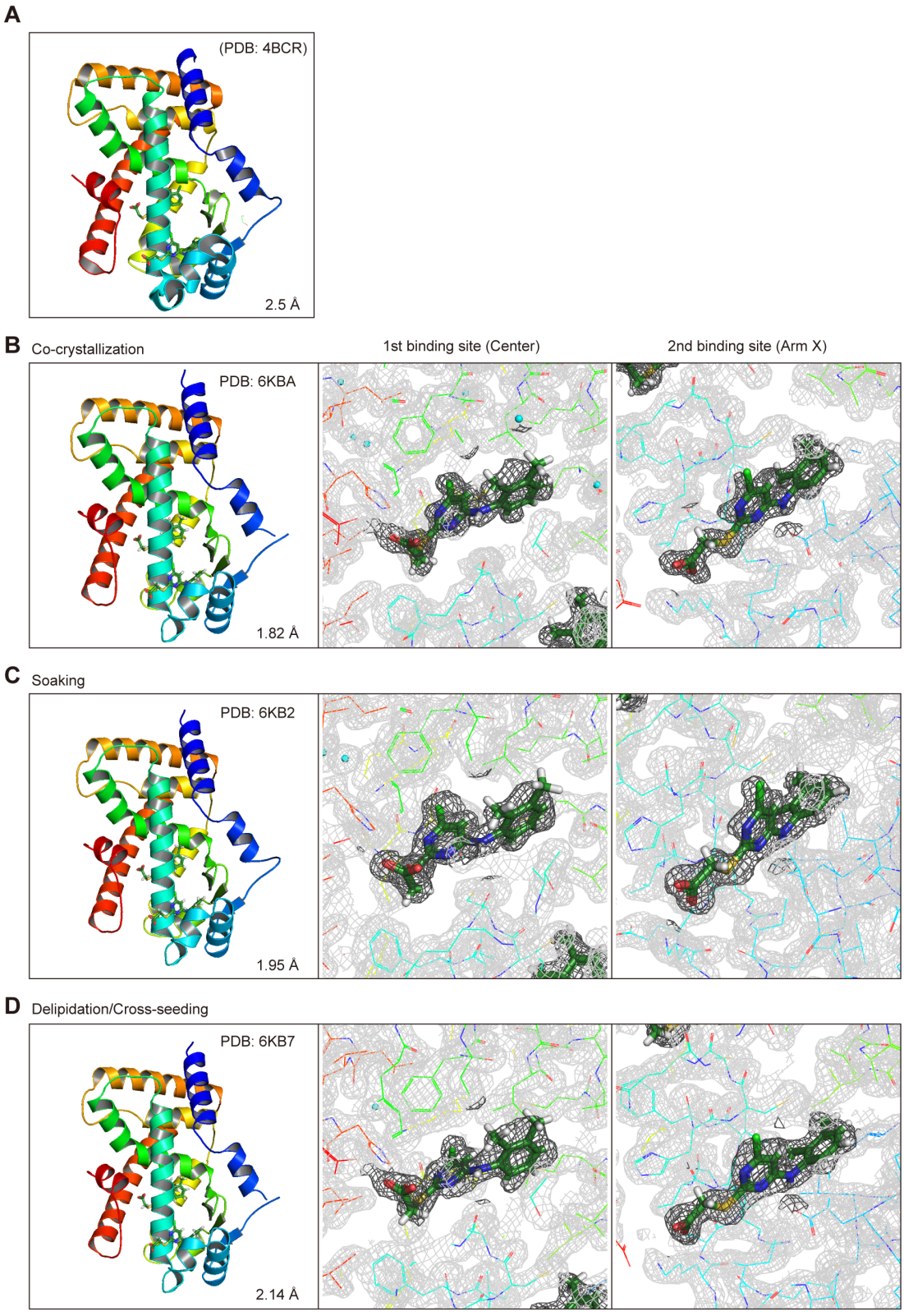

Figure S4. Crystal structures of PPARα-LBD bound to two Wy14643 molecules by different crystal preparation methods, Related to Figure 1

(A) PDB (ID: 4BCR): Deposited Wy14643 (×2)-bound structure deposited (Bernardes *et al.*, 2013). (B–D) Overall structures and magnified views of two Wy14643 binding sites, located in the Center and Arm X regions, in crystals obtained using co-crystallization (B), soaking (C), or delipidation/cross-seeding (D) procedures. The electron density is shown in the mesh using Feature Enhanced Maps (FEMs) contoured at 1.0σ. PDB identities and resolutions are labelled, and water molecules are presented as cyan spheres.

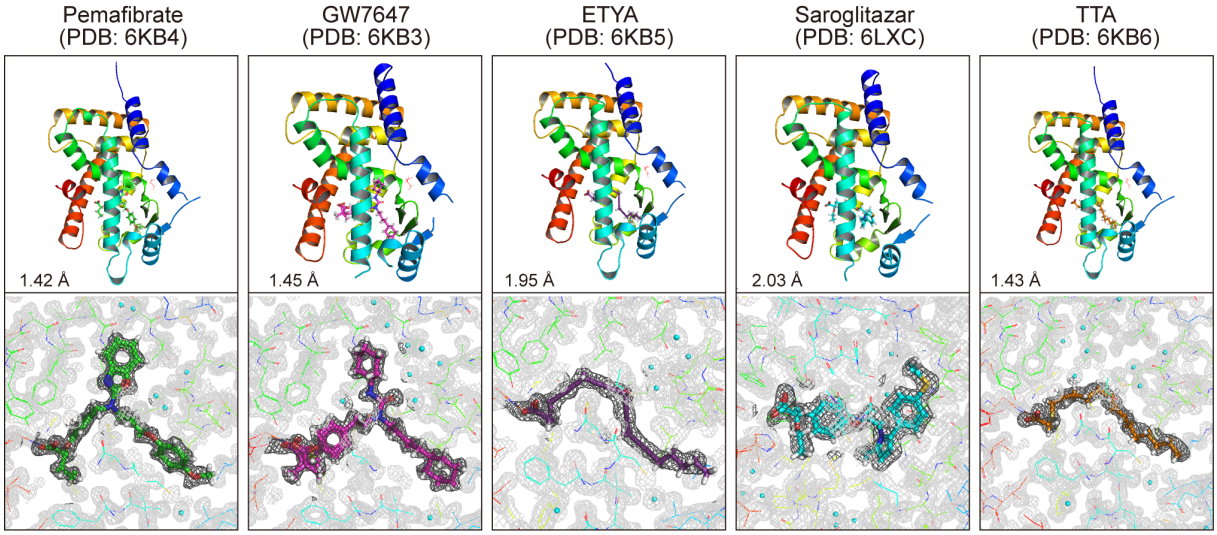

Figure S5. Crystal structures and magnified views of PPARα-LBD and five potent PPARα agonists obtained using cross-seeding of the delipidized proteins, Related to Figure 2

The electron density is shown in the mesh by FEMs contoured at 1.0σ. PDB identities and resolutions are labelled, and water molecules are presented as cyan spheres.

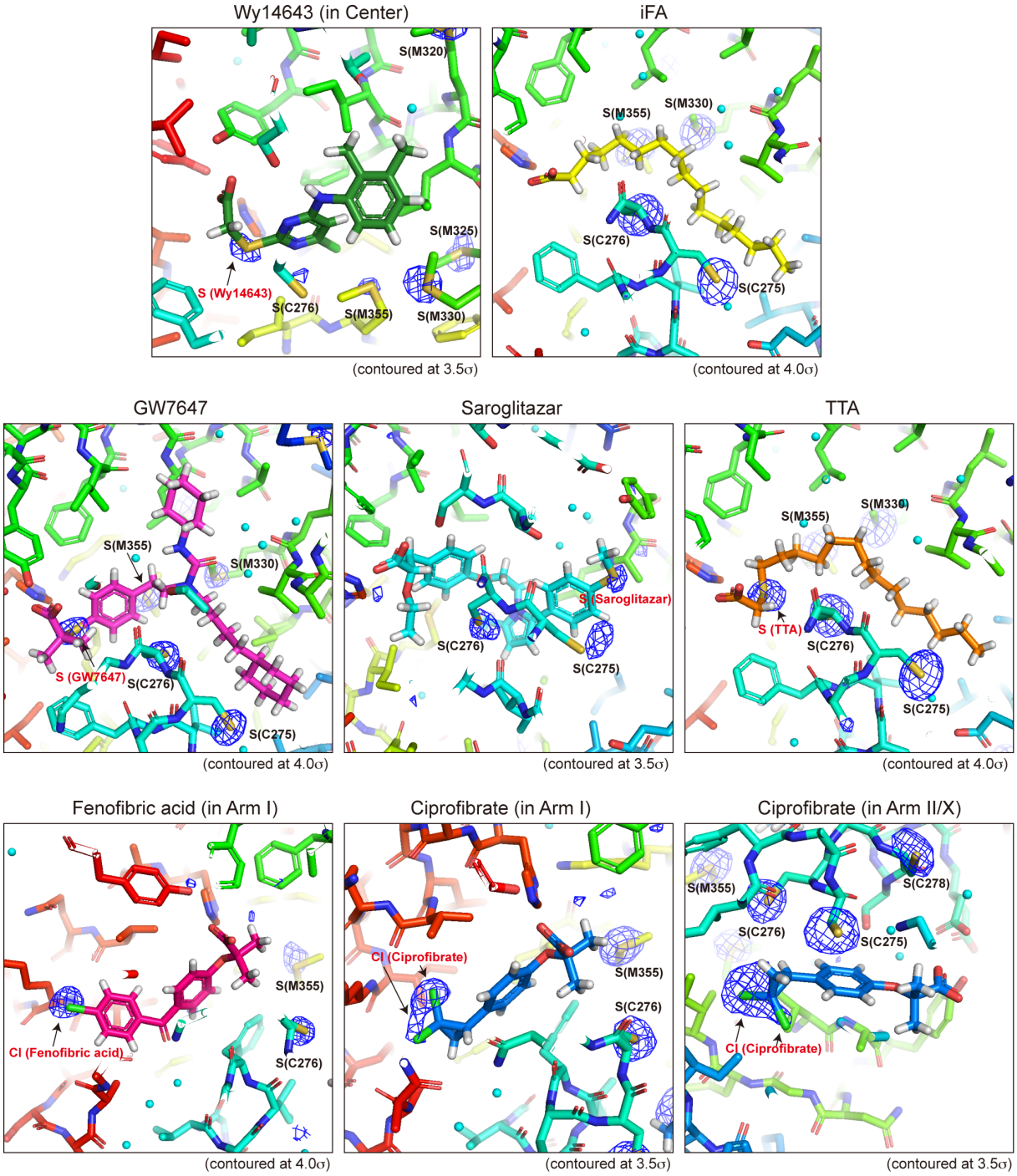

Figure S6. Magnified views of PPARα-LBD–ligand structures superimposed with sulfur/chloride signals located using anomalous difference Fourier maps, Related to Figure 2

PPARα agonists, such as Wy14643, GW7647, saroglitazar, and TTA, but not intrinsic fatty acid, have been found to possess single sulfur atoms in their molecules, which are detectable using anomalous difference Fourier maps, contoured at 3.5σ or 4.0σ, conducted with 1.8 Å X-ray. Chloride signals in fenofibric acid and ciprofibrate were also detected. The electron density is shown in the mesh, and water molecules are presented as cyan spheres. The locations of all the sulfur/chloride signals correspond to the signals revealed by routine 1.0 Å X-ray crystallography.

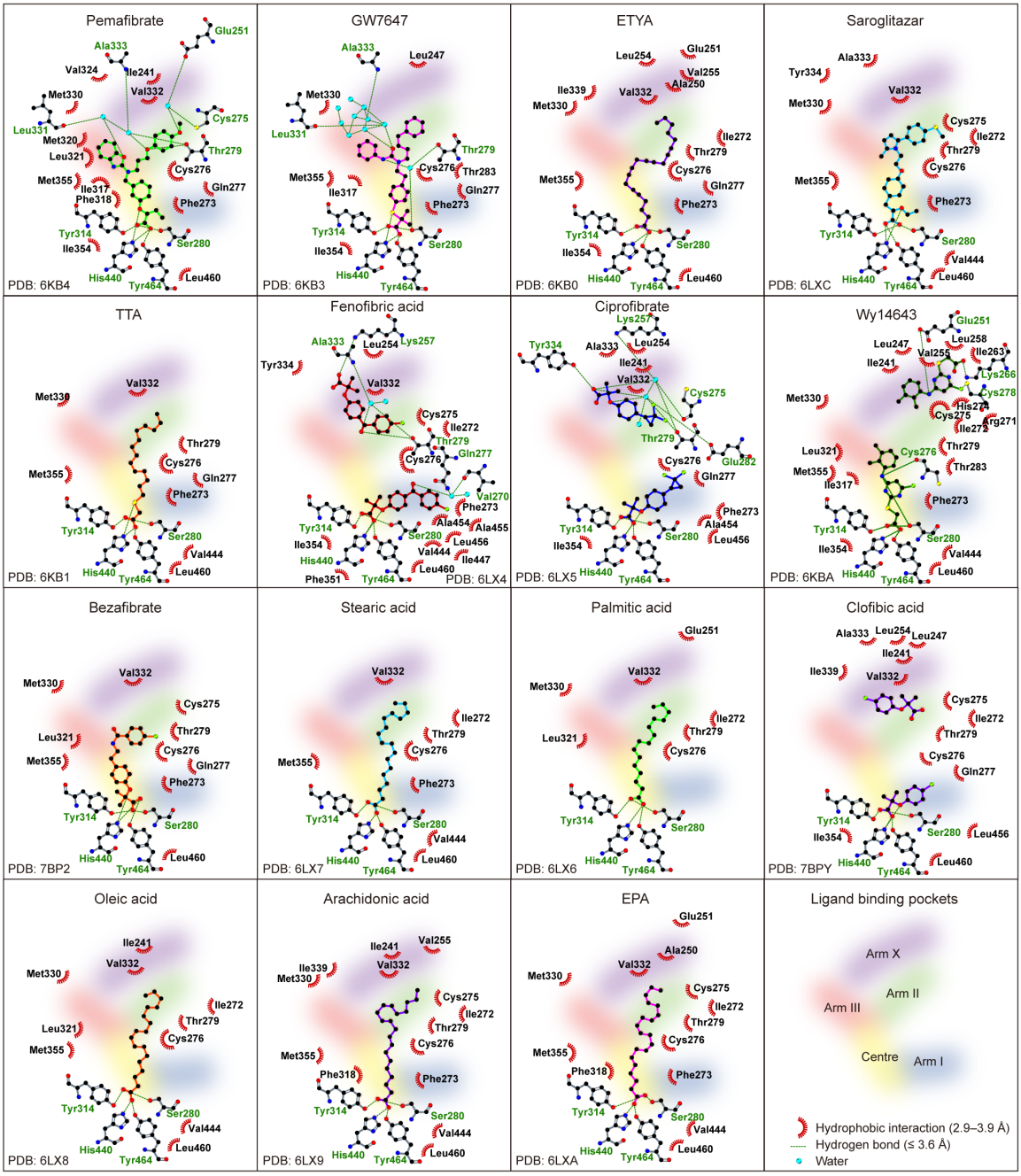

Figure S7. Interatomic interaction of 15 ligands with PPARα-LBDs, Related to Figures 2 and 3
Conserved hydrogen bonds, including those between the carboxyl groups of ligands and their surrounding S280, Y314, H440, and Y464 residues in Arm I/Center boundary, are illustrated by green dashed lines. All plots were generated using LigPlot+.

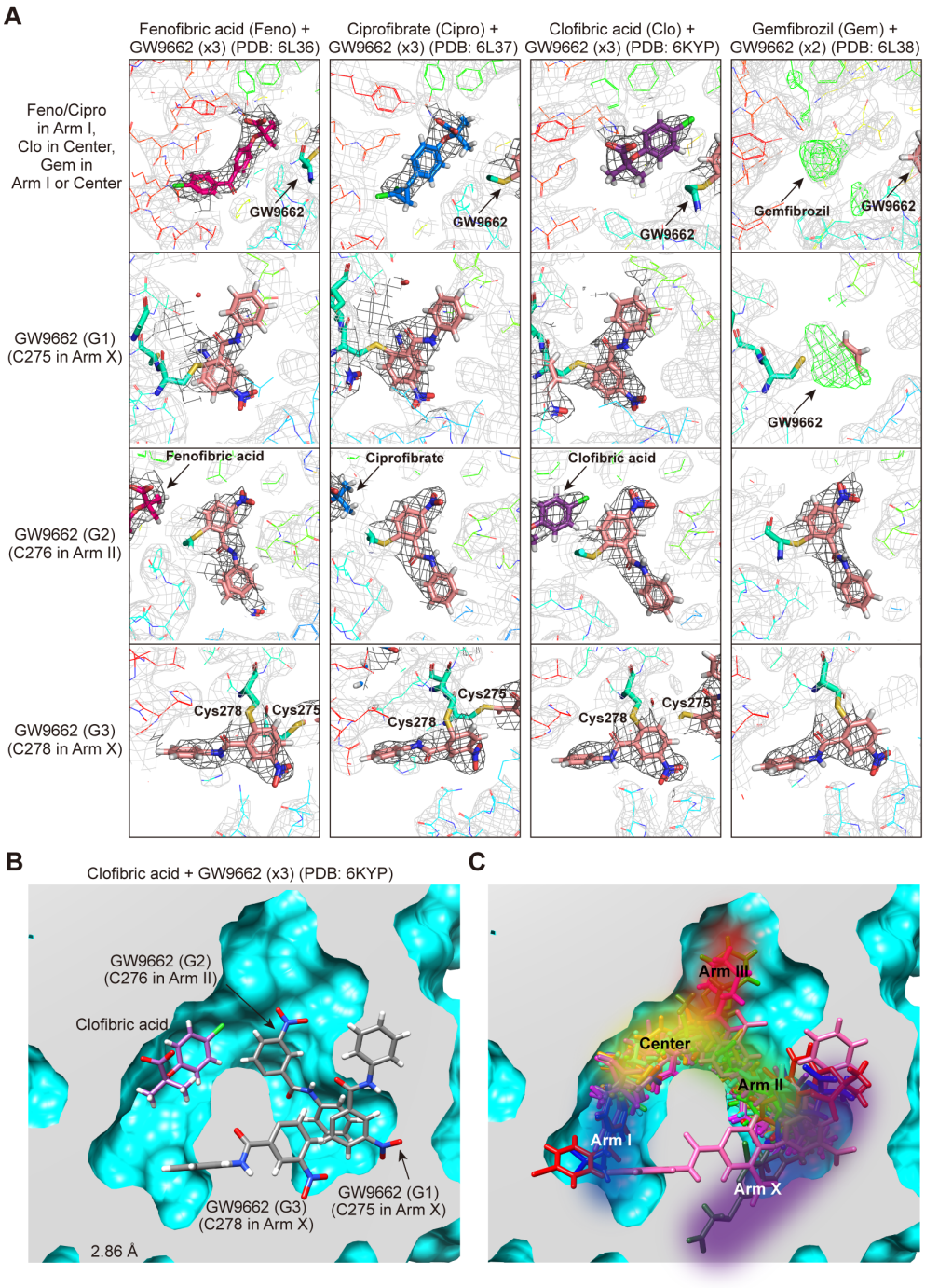

Figure S8. Magnified views of crystal structures of PPARα-LBD with fibrates and GW9662 and enlarged LBD spaces by this study, Related to Figure 4

(A) Fenofibric acid and ciprofibrate are located at Arm I (two sites, Arm I and II/X boundary, in the absence of GW9662), whereas three GW9662 are located at Arm II and X; one molecule is covalently bound to Cys276 in Arm II, and two molecules are covalently bound to Cys275 and Cys278 in Arm X. Clofibric acid is located at the Center or at Arm I in the absence of GW9662, and three GW9662 are located similarly. Although no crystals were obtained with gemfibrozil alone, crystals with combinations of gemfibrozil and GW9662 were acquired. Only unclear electron densities of gemfibrozil, in the Center, and single GW9662 molecule, attached to Cys275, were obtained, but two GW9662 were covalently bound to Cys276 in Arm II and Cys275 in Arm X, explicitly. The electron density is shown in the black mesh using FEMs contoured at 1.0σ and in the green mesh, only for gemfibrozil crystals, using *F*o-*F*c omit maps contoured at 3.0σ. (B) A magnified view of PPARα-LBD bound with clofibric acid/GW9662 (×3). (C) Enlarged PPARα-LBD spaces from the results of this study. Original spaces for four Arms and Center regions (the same in Figure S1B) are illustrated.

Table S1. Twenty-one PPARα-LBD X-ray crystal structures deposited so far in the Protein Data Bank (PDB) to date, Related to Table 1

PDB ID	Resolution	Ligand(s)	Publication	Released date
3VI8	1.75 Å	13M	*J. Med. Chem.* 55, 893–902 (2012)	2012/8/29
2P54	1.79 Å	735	*J. Med. Chem.* 50, 685–695 (2007)	2007/4/24
5HYK	1.83 Å	65W	*Sci. Rep.* 6, 34792 (2016)	2016/11/23
6KXX	1.95 Å	T02	*Sci. Rep.* 10, 4623 (2020)	2020/5/20
6KXY	2.00 Å	T06	*Sci. Rep.* 10, 4623 (2020)	2020/5/20
2ZNN	2.01 Å	S44	*Acta Crystallogr. D Biol. Crystallogr.* 65, 786–795 (2009)	2009/5/5
3KDU	2.07 Å	NKS	*J. Med. Chem.* 53, 2854–2864 (2010)	2010/4/28
1I7G	2.2 Å	AZ2	*Structure* 9, 699–706 (2001)	2002/3/9
3G8I	2.2 Å	RO7	*Bioorg. Med. Chem. Lett.* 19, 2468–2473 (2009)	2009/6/2
3SP6	2.21 Å	IL2	*J. Biol. Chem.* 286, 31473–31479 (2011)	2011/7/20
2NPA	2.3 Å	MMB	*Bioorg. Med. Chem. Lett.* 17, 937–941 (2007)	2007/10/30
4Cl4	2.3 Å	Y1N	*J. Struct. Biol.* 191, 332–340 (2015)	2014/12/24
2REW	2.35 Å	REW	Not published	2007/11/27
3FEI	2.4 Å	CTM	*ChemMedChem* 4, 951–956 (2009)	2009/10/20
1K7L	2.5 Å	544	*Proc. Natl. Acad. Sci. USA* 98, 13919–13924 (2001)	2001/12/5
3ET1	2.5 Å	ET1	*Proc. Natl. Acad. Sci. USA* 106, 262–267 (2009)	2009/2/17
4BCR	2.5 Å	WY1	*J. Mol. Biol.* 425, 2878 (2013)	2013/5/29
3KDT	2.7 Å	7HA	*J. Med. Chem.* 53, 2854–2864 (2010)	2010/4/28
1KKQ	3.0 Å	471	*Nature* 415, 813–817 (2002)	2002/2/20
6L96	3.20 Å	P7F	*Int. J. Mol. Sci.* 21, 361 (2020)	2020/1/6
5AZT	3.45 Å	4M5	*ACS Chem.Biol.* 11, 2447–2455 (2016)	2016/7/6

Data are ordered by the highest resolutions of crystal structures.

TRANSPARENT METHODS

Key Resources Table

REAGENT or RESOURCE	SOURCE	IDENTIFIER
Antibodies		
Eu-W1024-labelled anti-6×His antibody	PerkinElmer	Cat#AD0205; RRID: AB_2811261
Bacterial and Virus Strains		
Escherichia coli Rosetta (DE3) pLysS	Novagen	Cat#70956
Biological Samples		
Human blood	This paper	N/A
Chemicals, Peptides, and Recombinant Proteins		
Polyethyleneimine	Fujifilm-Wako	Cat#167-11951; CAS: 9002-98-6
d_{33}-Oleic acid	Cambridge Isotope Laboratories	Cat#DLM-1891-PK
Polyethylene glycol (PEG) 3,350	Hampton Research	Cat#HR2-144; CAS: 25322-68-3
SRC1 pentadecenoyl peptide (LTERHKILHRLLQEG)	GenScript	N/A
GW7647	Cayman Chemical	Cat#10008613; CAS: 265129-71-3
Bezafibrate	Cayman Chemical	Cat#10009145; CAS: 41859-67-0
Tetradecylthioacetic Acid	Fujifilm-Wako	Cat#209-18141; CAS: 2921-20-2
Wy14643	Cayman Chemical	Cat#70730; CAS: 50892-23-4
GW9662	Cayman Chemical	Cat#70785; CAS: 22978-25-2
Ciprofibrate	Fujifilm-Wako	Cat#033-21191; CAS: 52214-84-3
Fenofibric acid	Combi-Blocks	Cat#OR-1173; CAS: 42017-89-0
5, 8, 11, 14-Icosatetraynoic Acid	Cayman Chemical	Cat#90120; CAS: 1191-85-1
Icosapentaenoic Acid	Cayman Chemical	Cat#90110; CAS: 10417-94-4
Clofibric Acid	LKT Labs	Cat#C4556; CAS: 882-09-7
Gemfibrozil	Combi-Blocks	Cat#OR-0524; CAS: 25812-30-0
Arachidonic acid	Cayman Chemical	Cat#10006607; CAS: 6610-25-9
Pemafibrate	Chemscene	Cat# CS-6084; CAS: 848259-27-8
Saroglitazar	Chemscene	Cat# CS-6149; CAS: 495399-09-2
Myristic acid	Nacalai Tesque	Cat#23517-82; CAS: 544-63-8
Palmitic acid	Sigma-Aldrich	Cat#P0500-10G; CAS: 57-10-3
Stearic acid	Sigma-Aldrich	Cat#S4751-1G; CAS: 57-11-4
Oleic acid	Nacalai Tesque	Cat#25630-51; CAS: 112-80-1
Linoleic acid	Nacalai Tesque	Cat#20513-41; CAS: 60-33-3
α-Linolenic acid	Cayman Chemical	Cat#90210; CAS: 463-40-1
Vaccenic Acid	Sigma-Aldrich	Cat#V1131-100MG; CAS: 693-72-1

Biotin-labelled PGC1α peptides (biotin-EAEEPSLLKKLLLAPANTQ	GenScript	N/A
ULight-Streptavidin	PerkinElmer	Cat#TRF0102
Critical Commercial Assays		
NEFA C-test Wako	Fujifilm-Wako	Cat#279-75401
AMP+ mass spectrometry kit	Cayman Chemical	Cat#710000
Crystal Screen	Hampton Research	Cat#HR2-110
Crystal Screen 2	Hampton Research	Cat#HR2-112
Index	Hampton Research	Cat#HR2-144
PrimeSTAR mutagenesis basal kit	Takara Bio	Cat#R046A
Deposited Data		
34 novel hPPARα-LBD structures in this study	Protein Data Bank (PDB)	Table 1
21 hPPARα-LBD structures so far deposited in PDB	Protein Data Bank (PDB)	Table S1
Recombinant DNA		
pET28a encoding human PPARα residues 200–468	Oyama et al., 2009	N/A
Software and Algorithms		
XDS v-Jan 26 2018 or Mar 15 2019	Kabsch, 2010	http://xds.mpimf-heidelberg.mpg.de/; RRID: SCR_015652
Aimless v-0.5.21	Evans & Murshudov, 2013	https://www.ccp4.ac.uk/; RRID: SCR_015747
Phaser v-2.7.6	McCoy et al., 2007	https://www.ccp4.ac.uk/; RRID: SCR_014219
Phenix v-1.11.1-2575-000	Adams et al., 2010	https://www.phenix-online.org/; RRID: SCR_014224
Coot v-0.8.2	Emsley & Cowtan, 2004	https://www.ccp4.ac.uk/; RRID: SCR_014222
PyMOL v-1.8.x	Schrodinger	https://pymol.org/2/; RRID: SCR_000305
UCSF Chimera v-1.10.2	Pettersen et al., 2004	https://www.cgl.ucsf.edu/chimera/; RRID: SCR_004097
LigPlot+ v-1.4.5	Laskowski & Swindells, 2011	https://www.ebi.ac.uk/thornton-srv/software/LigPlus/; RRID: SCR_018249
GraphPad Prism v-5.0c	GraphPad Software	https://www.graphpad.com/scientific-software/prism/; RRID: SCR_002798
Other		
TALON Metal Affinity Resin	Clontech	Cat#635682
HiTrap Q	GE Healthcare	Cat#17115301
HiLoad 16/600 Superdex 75 pg gel-filtration column	GE Healthcare	Cat#28989333
Slide-A-Lyzer G2 Dialysis Cassette	Thermo Fisher	Cat#87735
Develosil HB-C30-UG 3 μm column, 100 × 2.0 mm	Nomura Chemical	Cat#HBUG173201001

PPARα-LBD expression and purification

Human PPARα-LBD (amino acids 200–468) was expressed as an amino-terminal His-tagged protein from a pET28a vector (Novagen) in Rosetta (DE3) pLysS competent cells (Novagen) and was purified by three-step chromatography (Capelli *et al.*, 2016; Oyama *et al.*, 2009) with some modifications. Transformed cells were cultured in LB medium (with 15 μg/ml kanamycin and 34 μg/ml chloramphenicol) at 30 °C, and 50 mL of overnight culture was seeded in 1 L of TB medium (with 15 μg/ml kanamycin), which was cultured at 30 °C for 1.5 h and then at 15 °C for 2 h. Protein overexpression was induced by adding 0.5 mM isopropyl β-D-galactopyranoside, which was later cultured at 15 °C for 48 h. The cells were harvested and resuspended in 40

mL buffer A (20 mM Tris-HCl (pH 8.0), 150 mM NaCl, 1 mM Tris 2-carboxyethylphosphine (TCEP)-HCl, and 10% glycerol) containing a cOmplete EDTA-free protease inhibitor (Sigma-Aldrich). The cells were then lysed by sonication for 2 min five times at an output of 8 with a UD-201 sonicator (Tomy, Tokyo, Japan) and clarified using centrifugation at 12,000 *g*, for 20 min, at 4 °C (the same conditions were used subsequently unless otherwise noted), and polyethyleneimine was added with a final concentration of 0.15% (v/v) to the supernatant in order to remove nucleic acids. After centrifugation, 35 ml of the supernatant was mixed with 20 g of ammonium sulfate at 4 °C for 30 min using gentle rotation. After centrifugation, the pellet was resuspended in 30 mL of buffer B, which was buffer A plus 10 mM imidazole. The suspension was loaded on a cobalt-based immobilized metal affinity column (TALON Metal Affinity Resin, Clontech), equilibrated with buffer B, and eluted with a linear gradient of 10–100 mM imidazole. The PPARα-LBD-containing elutes (e.g., fraction nos. 5–10 in Figure S3B, left) were incubated with 33 U/ml thrombin protease (Nacalai Tesque, Kyoto, Japan) to cleave His tag and, at the same time, dialyzed against buffer A overnight at 4 °C using a Slide-A-Lyzer G2 Dialysis Cassette (20-kDa cutoff, Thermo Fisher Scientific). Then, the sample was later dialyzed against buffer C, which was buffer A minus 150 mM NaCl, at 4 °C for 3 h. The sample was then loaded onto a HiTrap Q anion-exchange column (GE Healthcare), equilibrated with buffer C, and eluted with a linear gradient of 0–150 mM NaCl. The elutes (e.g., fraction nos. 6–7 in Figure S3B, right) were loaded onto a HiLoad 16/600 Superdex 75 pg gel-filtration column (GE Healthcare), equilibrated with buffer A, and eluted with buffer A. The purity of human PPARα-LBD was continuously analyzed using SDS-PAGE and Coomassie Brilliant Blue staining (Figure S3B).

Measurement of fatty acid contents in PPARα-LBD and human serum

The total free fatty acid levels in PPARα-LBD proteins were measured using the NEFA C-test Wako for *in vitro* diagnosis (Fujifilm-Wako, Osaka, Japan). To analyze their contents, a 10 µl aliquot of PPARα-LBD proteins (20 mg/ml) was transferred to a clean glass tube containing 100 pmol d33-oleic acid as an internal standard. Lipids were extracted using Bligh & Dyer methods (Bligh & Dyer, 1959). Then 30 µl of chloroform/methanol (1:2, v/v) was added and mixed well. Next, 10 µl of chloroform and then 10 µl of water were added to the samples, which were mixed well, and centrifuged at 3,000 *g*, for 5 min, at room temperature. Then, the lower organic phase was transferred to another glass tube and dried under a stream of argon gas. Free fatty acids were derivatized with *N*-(4-aminomethylphenyl)pyridinium (AMPP) using a AMP+ mass spectrometry kit (Cayman Chemical) as previously reported (Bollinger *et al.*, 2013). Briefly, the samples were resuspended in 5 µl ice-cold acetonitrile/dimethylformamide (4:1, v/v), and the following reagents were added: 5 µl of 640 mM 1-ethyl-3-(ε-dimethylaminopropyl)carbodiimide in water, 2.5 µl of 20 mM *N*-hydroxylbenzotriazole in acetonitrile/dimethylformamide 99:1, and 7.5 µl of 20 mM AMPP in acetonitrile. Then, the samples were mixed, incubated at 60 °C for 30 min, and analyzed on the same day.

The collection and lipid analyses of blood/serum were approved (no. 2019-5) by the Ethics Committee of Showa Pharmaceutical University with informed consent from all participants, and personal information was blinded to the experimenters. For the analysis of fatty acid contents in human serum, 8 µl aliquot of serum was transferred to a clean glass tube. Reagents were added to each tube: 2 µl of 4 mM d33-oleic acid, as an internal standard, 90 µl of water, 200 µl of chloroform, and 400 µl of methanol. The samples were mixed well. Then, 200 µl of chloroform and later 300 µl of water were added, mixed well, and centrifuged at 3,000 *g*, for 5 min, at room temperature. The lower organic phase was transferred to another glass tube and dried under a stream of argon gas.

Fatty acids in human plasma were also derivatized using the mass spectrometry kit. The samples were resuspended in 30 µl of ice-cold acetonitrile/dimethylformamide (4:1, v/v), and 20 µl of 640 mM 1-ethyl-3-(ε-dimethylamino-propyl)carbodiimide in water, 10 µl of 20 mM *N*-hydroxylbenzotriazole in acetonitrile/dimethylformamide 99:1, and 20 µl of 20 mM AMPP in acetonitrile were added. The samples were briefly mixed, incubated at 60 °C for 30 min, and analyzed on the same day.

Mass spectrometric analyses were performed using a Waters Xevo TQD triple quadrupole mass spectrometer interfaced to an ACQUITY ultra-performance liquid chromatography (UPLC) system (Waters). UPLC was carried out using a reverse-phase C30 column (Develosil HB-C30-UG 3-µm column, 100 × 2.0 mm, Nomura Chemical, Aichi, Japan). Solvent A was water containing 0.1% formic acid, and solvent B was acetonitrile containing 0.1% formic acid. The solvent program included linear gradients: 40% of solvent B at 0 min, 99% of solvent B at 8–10 min, and 40% of solvent B at 10.1 min. The flow rate was 0.3 ml/min, and the column temperature was set at 40 °C. Selected reaction monitoring (SRM) was performed in the positive ion mode using nitrogen as the nebulizing gas. The monitored SRM transitions were as follows: myristic acid, *m*/*z* 395.0 > 239.0; palmitic acid, *m*/*z* 423.0 > 239.0; stearic acid, *m*/*z* 451.0 > 239.0; oleic acid, *m*/*z* 449.0 > 239.0; linoleic acid, *m*/*z* 447.0 > 239.0; linolenic acid, *m*/*z* 445.0 > 239.0; arachidonic acid, *m*/*z* 471.0 > 239.0; and d33-oleic acid, *m*/*z* 482.6 > 242.3. The amounts of fatty acid derivatives were calculated using the ratios of the peak area of the target compounds and of the derivatized stable isotope (d33-oleic acid). MassLynx version 4.1 was used for the system control and data processing.

Delipidation of PPARα-LBD

The PPARα-LBD-containing elutes from the cobalt column were precipitated with 9× volumes of ethanol for 2 h at room temperature. After centrifugation at 15,000 *g* for 10 min at 4 °C, the pellet was washed twice using 90% ethanol, and resuspended in 20 mL of 6 M guanidinium hydrochloride in buffer A overnight at 4 °C. For refolding, the sample was directly diluted with 180 mL of buffer A and then concentrated by centrifugation to 3 mL using an Amicon Ultra-15 centrifugal filter (3-kDa cutoff, Merck Millipore). Thereafter, the sample was treated with thrombin and dialyzed with buffer A and was processed as described above.

Co-crystallization and soaking

After examining 192 different buffer conditions using the Crystal Screen and Crystal Screen 2, and Index crystallization kits from Hampton Research at 4 °C and 20 °C (Table S2), we were able to obtain characteristic rod-shaped Wy14643-bound crystals (Figure 1A) in 0.1 M Bis-Tris (pH 6.5)/25% (w/v) polyethylene glycol (PEG) 3,350 (no. 43 buffer in the Index kit) at 4 °C using co-crystallization, which gave a 1.82 Å resolution structure (Crystal no.15 in Table S3). Following this method, co-crystallization was performed in hanging-drop mixtures of 0.5 µl PPARα-LBD (20 mg/ml in buffer A), 0.5 µl ligand (200–2,000 µM in buffer A), and 1 µl reservoir solution (variations of no. 43 buffer: 0.1 M Bis-Tris (pH 6.5), 0.1 M HEPES (pH 7.0 or 7.5), or 0.1 M Tris (pH 8.0 or 8.5) with 25% PEG 3,350) at 4 °C for several weeks. To prepare the PPARα-LBD/ligand/coactivator crystals, 0.25 µl ligand (2 mM in buffer A) and 0.25 µl SRC1 pentadecenoyl peptide (LTERHKILHRLLQEG synthesized by GenScript) were used instead of the 0.5 µl ligand above. For the cross-seeding, Wy14643-bound crystals were crushed using small needles in the reservoir solution. Then, the crushed crystal powder was transferred to another PPARα-LBD/(another) ligand/reservoir solution using a single streak with a human crown

hair, and this was incubated at 4 °C for several weeks. For soaking, iFA-bound PPARα-LBD crystals were soaked in a reservoir solution (0.1 M HEPES (pH 7.5), 20% PEG 3,350) containing 0.5–5 mM ligand (final 0.1–1% DMSO) at 4 °C for several weeks. All crystals were briefly soaked in cryoprotection buffer (their respective reservoir solutions with 20% glycerol); afterwards, these were flash-cooled in a stream of liquid nitrogen until X-ray crystallography was conducted.

X-ray diffraction data collection and model refinement

Datasets were collected at four available beamlines (BL-5A, BL-17A, and AR-NE3A at the Photon Factory (Ibaraki, Japan) and BL26B1 at the SPring-8 (Hyogo, Japan)) using synchrotron radiation of 1.0 Å. X-ray diffraction data were also collected using 1.8 Å wavelength X-ray to identify sulfur and chloride atoms in some ligands by analyzing anomalous scattering signals included in X-ray diffraction data (Liu *et al.*, 2012). Although sulfur and chloride atoms have the absorption K-edge at wavelengths longer than 1.8 Å, the anomalous difference Fourier maps exhibited significant signals, which enabled to locate those atoms within the crystal structures. Diffraction data was collected at 0.1˚ oscillation per frame, and a total of 1,800 frames (180˚) were recorded for 1.0 Å X-ray crystallography and 3,600 (360˚) frames for 1.8 Å crystallography. Data processing and scaling were carried out using XDS X-ray detector software (Kabsch, 2010) and AIMLESS (Evans & Murshudov, 2013), respectively. Resolution cutoff values (R_{merge} < 0.5, R_{pim} < 0.3, and Completeness < 0.9) were set by the highest resolution shell. All structures were determined using molecular replacement in PHASER (McCoy *et al.*, 2007) and 1.75 Å resolution structures of synthetic ligand-containing human PPARα-LBD (PDB: 3VI8) (Table S1) as the starting model. Refinement of the structure was performed using iterative cycles of model adjustment in two programs: COOT (Emsley & Cowtan, 2004) and PHENIX (Adams *et al.*, 2010). All collection data and refinement statistics are included in Tables S3 and S4, and essential data are shown in Table 1 with web links to the PDB. *F*o-*F*c omit maps and Feature Enhanced Maps (FEMs) were calculated using PHENIX. The structures were constructed using PyMOL (http://www.pymol.org) and USCF Chimera (Pettersen *et al.*, 2004) programs. The interatomic interaction of ligands with PPARα-LBDs was investigated using LigPlot+ (Laskowski & Swindells, 2011).

PPARα activation (PGC1α coactivator recruitment) assay

Activation/inactivation status of PPARα can be determined using a time-resolved fluorescence resonance energy transfer (TR-FRET) assay, which is used for detecting physical interactions between His-tagged human PPARα-LBD proteins and biotin-labelled PGC1α coactivator peptides (biotin-EAEEPSLLKKLLLAPANTQ synthesized by GenScript) using a LANCE Ultra TR-FRET Assay (PerkinElmer). For the activation assay, 9.5 µl of PPARα-LBD (200 nM in buffer D (10 mM HEPES-HCl (pH7.4), 150 mM NaCl, 0.005% Tween 20, 0.1% fatty acid-free bovine serum albumin)), 0.5 µl of 100× ligand solution (in DMSO or ethanol), and 5 µl of biotin-PGC1α peptide (4 µM) were mixed in a single well of a Corning 384 well low volume white round bottom polystyrene non-binding surface microplate. Then, 5 µl of 4 nM Eu-W1024-labelled anti-6×His antibody (PerkinElmer)/80 nM ULight-Streptavidin (PerkinElmer) was added to each well and the microplate was incubated in the dark at room temperature for 2 h. FRET signals were detected at one excitation filter (340/12) and two emission filters (615/12 and 665/12) using the Varioskan Flash double monochromater microplate reader (Thermo Fisher Scientific). The parameters for the measurement at 615 nm and 665 nm were an integration time of 200 µs and a

delay time of 100 μs. The 665 nm emissions were due to ULight-FRET, and the 615 nm emissions were due to Eu-W1024. The 665/615 ratio was calculated and normalized to the negative control reaction using 1% DMSO. For the inactivation assay, graded concentrations of GW9662 were added in the presence of 1–3,000 μM of ligand. Nonlinear fitting and calculation of EC_{50} and IC_{50} were performed using Prism 5 software (GraphPad, San Diego, USA).

Thermostability assay using CD spectroscopy

Around 10 μM of the PPARα-LBD proteins was incubated with varied concentrations of ligands in buffer A. The CD spectra were monitored within 200–260 nm at increasing temperatures from 30 °C to 70 °C (2 °C/min) with the use of a J-1500 spectropolarimeter (JASCO, Tokyo, Japan), which is equipped with a PTC-510 thermal controller (JASCO). Approximate melting temperatures were obtained by fitting a single-site sigmoidal dose response curve using Prism 5.

Mutagenesis of PPARα-LBD cDNA

Site-directed mutagenesis (single amino acid substitutions) was performed using a PrimeSTAR Mutagenesis Basal Kit (Takara Bio). The Cys275Ser (C275S) and C276S but not C278S PPARα-LBD mutants displayed ligand-dependent activation (coactivator recruitment).

Quantification and Statistical Analysis

Data are presented as means ± SEM (*n*: numbers of independent experiments that have 3–4 well replicates) or means ± SD for the human samples. Statistical comparison was performed using an unpaired two-tailed Student's *t*-test in Prism 5. All *P*-values <0.05 denote a significant difference.

References

Adams, P.D., Afonine, P.V., Bunkóczi, G., Chen, V.B., Davis, I.W., Echols, N., Headd, J.J., Hung, L.W., Kapral, G.J., Grosse-Kunstleve, R.W., et al. (2010). PHENIX: a comprehensive Python-based system for macromolecular structure solution. Acta Crystallogr. D Biol. Crystallogr. *66*, 213–221.

Bernardes, A., Souza, P.C., Muniz, J.R., Ricci, C.G., Ayers, S.D., Parekh, N.M., Godoy, A.S., Trivella, D.B., Reinach, P., Webb, P., et al. (2013). Molecular mechanism of peroxisome proliferator-activated receptor alpha activation by WY14643: a new mode of ligand recognition and receptor stabilization. J. Mol. Biol. *425*, 2878–2893.

Bligh, E.G., and Dyer, W.J. (1959). A rapid method of total lipid extraction and purification. Can. J. Biochem. Physiol. *37*, 911–917.

Bollinger, J.G., Naika, G.S., Sadilek, M., and Gelb, M.H. (2013). LC/ESI-MS/MS detection of FAs by charge reversal derivatization with more than four orders of magnitude improvement in sensitivity. J. Lipid Res. *54*, 3523–3530.

Capelli, D., Cerchia, C., Montanari, R., Loiodice, F., Tortorella, P., Laghezza, A., Cervoni, L., Pochetti, G., and Lavecchia, A. (2016). Structural basis for PPAR partial or full activation revealed by a novel ligand binding mode. Sci. Rep. *6*, 34792.

Emsley, P., and Cowtan, K. (2004). Coot: model-building tools for molecular graphics. Acta Crystallogr. D Biol. Crystallogr. *60*, 2126–2132.

Evans, P.R., and Murshudov, G.N. (2013). How good are my data and what is the resolution? Acta Crystallogr. D Biol. Crystallogr. *69*, 1204–1214.

Kabsch, W. (2010). XDS. Acta Crystallogr. D Biol. Crystallogr. *66*, 125–132.

Kawasaki, M., Kambe, A., Yamamoto, Y., Arulmozhiraja, S., Ito, S., Nakagawa, Y., Tokiwa, H., Nakano, S., and Shimano, H. (2020). Elucidation of molecular mechanism of a selective PPARalpha modulator, pemafibrate, through combinational approaches of X-ray crystallography, Thermodynamic analysis, and first-principle calculations. Int. J. Mol. Sci. *21*, 361.

Laskowski, R.A., and Swindells, M.B. (2011). LigPlot+: multiple ligand-protein interaction diagrams for drug discovery. J. Chem. Inf. Model. *51*, 2778–2786.

Liu, Q., Dahmane, T., Zhang, Z., Assur, Z., Brasch, J., Shapiro, L., Mancia, F., and Hendrickson, W.A. (2012). Structures from anomalous diffraction of native biological macromolecules. Science *336*, 1033–1037.

McCoy, A.J., Grosse-Kunstleve, R.W., Adams, P.D., Winn, M.D., Storoni, L.C., and Read, R.J. (2007). Phaser crystallographic software. J. Appl. Crystallogr. *40*, 658–674.

Oyama, T., Toyota, K., Waku, T., Hirakawa, Y., Nagasawa, N., Kasuga, J.I., Hashimoto, Y., Miyachi, H., and Morikawa, K. (2009). Adaptability and selectivity of human peroxisome proliferator-activated receptor (PPAR) pan agonists revealed from crystal structures. Acta Crystallogr. D Biol. Crystallogr. *65*, 786–795.

Pettersen, E.F., Goddard, T.D., Huang, C.C., Couch, G.S., Greenblatt, D.M., Meng, E.C., and Ferrin, T.E. (2004). UCSF Chimera--a visualization system for exploratory research and analysis. J. Comput. Chem. *25*, 1605–1612.